

Rene: A Pre-trained Multi-modal Architecture for Auscultation of Respiratory Diseases

Pengfei Zhang¹, Zhihang Zheng¹, Shichen Zhang¹, Minghao Yang¹ and Shaojun Tang^{1,2*}

1. Bioscience and Biomedical Engineering Thrust, Systems Hub, The Hong Kong University of Science and Technology (Guangzhou), Guangzhou, Guangdong, China.
2. Division of Emerging Interdisciplinary Areas, The Hong Kong University of Science and Technology, Clear Water Bay, Hong Kong, SAR, China.

*E-mail: Correspondence: shaojuntang@ust.hk

ABSTRACT

This study presents a novel methodology utilizing a pre-trained speech recognition model for processing respiratory sound data. By incorporating medical record information, we introduce an innovative multi-modal deep-learning architecture, named Rene, which addresses the challenges of poor interpretability and underperformance in real-time clinical diagnostic response observed in previous respiratory disease-focused models. The proposed Rene architecture demonstrated significant improvements of 10.24%, 16.15%, 15.29%, and 18.90% respectively, compared to the baseline across four tasks related to respiratory event detection and audio record classification on the SPRSound database. In patient disease prediction tests on the ICBHI database, the architecture exhibited improvements of 23% in the mean of average score and harmonic score compared to the baseline. Furthermore, we developed a real-time respiratory sound discrimination system based on the Rene architecture, featuring a dual-thread design and compressed model parameters for simultaneous microphone recording and real-time dynamic decoding. Employing state-of-the-art Edge AI technology, this system enables rapid and accurate responses for respiratory sound auscultation, facilitating deployment on wearable clinical detection devices to capture incremental data, which can be synergistically evolved with large-

scale models deployed on cloud servers for downstream tasks.

KEYWORDS

Respiratory Sound Data Analysis, Multi-modal Fusion, Edge Artificial Intelligence

INTRODUCTION

The global prevalence of pulmonary diseases, especially the recent outbreak of COVID-19, highlights the growing importance of timely detection and effective diagnosis of pneumonia. This study systematically analyzes pulmonary audio signals using audio processing techniques to achieve robust pneumonia diagnosis. Pulmonary audio signals contain valuable physiological information, and their analysis can help identify pathological manifestations of pneumonia. For example, research has shown that patients in early-stage pneumonia exhibit increased respiratory audio frequencies, concentrating energy in the high-frequency range^[1]. This indicates airway narrowing, obstruction, and the presence of pulmonary inflammation, such as respiratory movement, airway constriction, and pulmonary effusion.

Analyzing these audio-derived physiological features enables a deeper understanding of pneumonia's pathological mechanisms, establishing a causal relationship between pulmonary audio signal characteristics and the disease. Furthermore, the deconvolution of audio data provides a theoretical foundation for pneumonia diagnosis and treatment. By leveraging various audio processing techniques, we can process pulmonary audio signals, extract embedded information, and develop reliable and efficient diagnostic tools and therapeutic devices for improved pneumonia diagnosis and treatment.

The fundamental principle of personalized lung sound assessment involves auscultation with a stethoscope placed on the chest. Normal lung auscultation produces two types of sounds: breath sounds and adventitious sounds^[2]. Breath sounds originate from airflow during respiration, while lung resonant sounds arise from gas resonance within the alveoli and bronchi. Generally, tracheal breath sounds are created by airflow passing through the trachea, yielding louder and clearer sounds. Conversely, bronchial breath sounds occur when airflow is obstructed in the bronchi, leading to weaker and less distinct sounds^[3].

Doctors can use a stethoscope's auscultation head to listen to various lung sounds and identify potential abnormalities. For example, inflammation or congestion in the lungs may produce crackles, which are typically moist sounds caused by fluid

accumulation in the alveoli and bronchi, obstructing normal airflow. Conversely, the presence of a tumor or foreign object in the airways can generate loud and harsh sounds^[4].

With the rapid advancement of artificial intelligence (AI) technology, there is growing interest in using deep learning for pneumonia detection and diagnosis based on audio data and medical imaging. Asif et al. developed a lightweight convolutional neural network (CNN) architecture using chest X-ray images from 2,541 confirmed COVID-19 cases and healthy controls across two public databases. Their model reliably detected COVID-19-infected patients through chest X-ray images^[5]. Jain et al. compared the accuracy of Inception V3, Xception, and ResNeXt models in chest X-ray scans of COVID-19 patients and healthy individuals using the posteroanterior (PA) view, systematically evaluating their performance and accuracy^[6]. Meanwhile, Mahmud proposed an effective solution for detecting COVID-19 cases even with small available X-ray sizes by efficiently utilizing trained parameters^[7].

As lung sound discrimination is a commonly used non-invasive method for pulmonary examination, audio processing techniques have been widely applied in pulmonary disease analysis. For instance, Imran's research demonstrated that machine learning algorithms can analyze COVID-19 pneumonia patients' cough sounds, enabling rapid detection and diagnosis^[8]. Chang et al. designed a simple homemade stethoscope to digitize medical sound data and analyzed the sounds to provide preliminary diagnoses and track health conditions^[9]. In the future, audio processing techniques are expected to play an increasingly important role in pneumonia detection and diagnosis.

The motivation for designing a multi-modal system stems from the understanding that relying solely on a simple model for disease diagnosis in a clinical context is insufficient. By leveraging multiple information sources, such as lung sounds and medical record data, diagnoses become more robust, rational, and interpretable. While lung sounds offer valuable insights into respiratory system functionality and disease states, relying exclusively on them may be limited due to factors like lung anatomy and respiratory strength. Integrating lung sounds with complementary information allows for a comprehensive diagnostic assessment, facilitating a holistic understanding of the patient's condition.

Incorporating clinical records, including vital history, symptoms, signs, and other relevant details, is crucial for accurate diagnoses and prognostication of disease progression. Fusing medical data with lung audio data enhances the reliability, precision, and interpretability of diagnoses, empowering clinicians to make informed decisions.

Adopting a multi-modal AI system enables the synergistic use of diverse information sources, improving the reliability and interpretability of diagnoses, and ultimately providing comprehensive support for clinical decision-making.

In this paper, we present Rene, a multi-modal lung sound analysis architecture named after Rene Laennec, the inventor of the stethoscope. We discuss Rene's performance on two publicly available databases, highlighting its effectiveness and accuracy in detecting respiratory sound events, identifying pathological patterns, and diagnosing patients. We then describe the development of a real-time sound processing system for auscultation flow audio using a dual-thread approach. This system is trained on a combined database using the Rene architecture and deployed on the auscultation device terminal, representing an edge artificial intelligence solution for monitoring respiratory system diseases.

RESULTS

The pipeline of Rene architecture

Our proposed Rene architecture is centered around the idea of multi-modal fusion diagnosis, with the flow chart illustrated in Figure 1A. This architecture comprises two primary modules, each dedicated to handling specific types of patient data to enhance the diagnostic process.

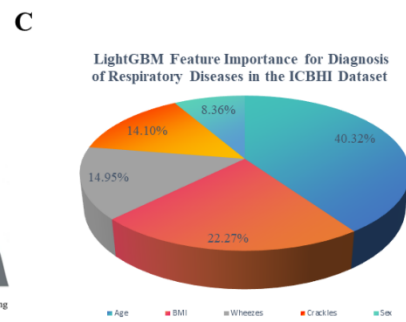
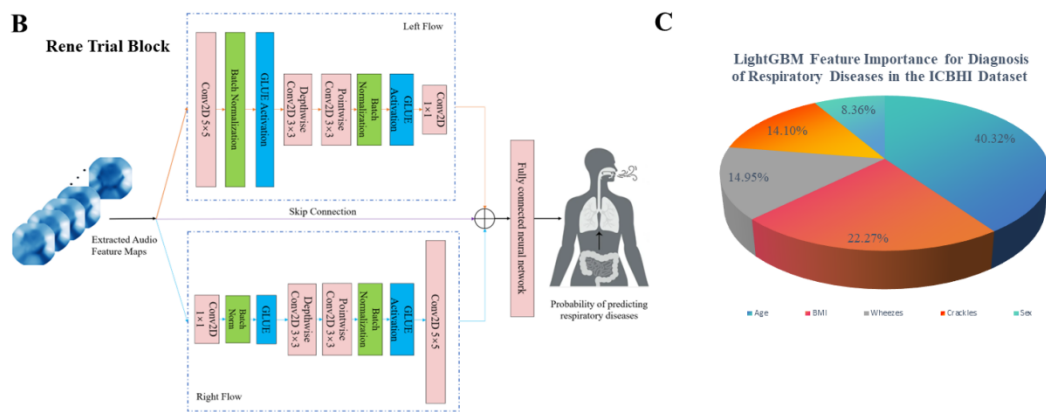
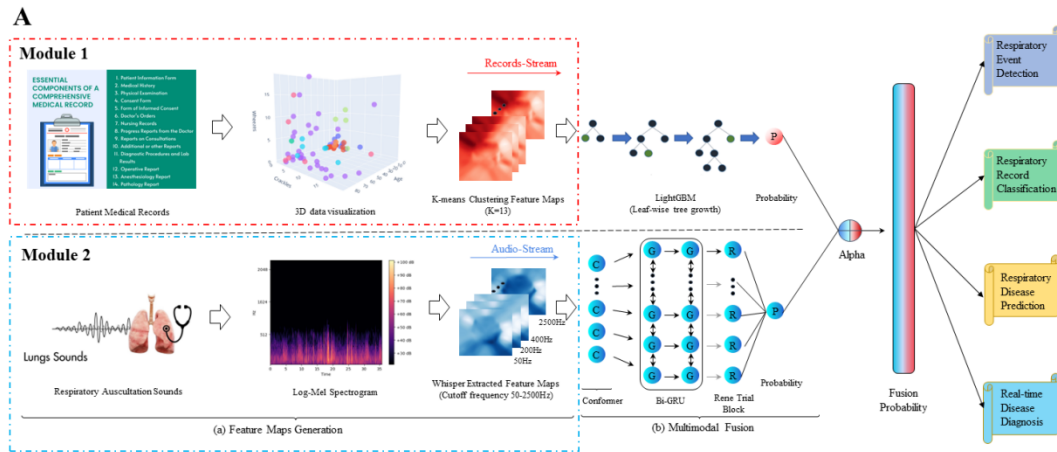


Fig. 1. (A) Overview of Rene architecture. Module 1 shows the steps of Rene architecture for feature map extraction of structured information in medical records. Module 2 demonstrates the operation method of the Rene architecture for lung sound extraction feature maps. **(B) The structure of Rene Trial Block.** The triadic branch jump design progressively constricts the left bypass receptive field while broadening the right flow. Integrating residual connections within the central pathway facilitates the preservation of original features. This enhances the network's learning process, fostering stability and smoothness. **(C) Comparison of information gain for Diagnosis of Respiratory Diseases.** We employed the LightGBM algorithm to calculate the gain importance of the electronic medical records from the ICBHI Respiratory Sound Database. This quantification revealed how specific features enhance model accuracy when used for segmentation. Consequently, we could discern the relevance of key features in predicting respiratory diseases, thereby amplifying the model's interpretability and predictive precision.

Module 1 is designed to extract features from patients' structured medical record data. It achieves this by employing 3D data visualization techniques, which allow for the observation of the distribution of various feature groups within the dataset. This comprehensive visualization enables the identification of patterns and correlations that might otherwise be difficult to discern. Following this step, the K-means clustering

algorithm^[10] is applied to extract intra-group features, effectively segmenting the data into meaningful clusters. This procedure culminates in the creation of an electronic medical record (EMR) feature map, which serves as a valuable diagnostic tool and reference point.

Module 2 is responsible for handling feature extraction and preprocessing of lung sound data. To accomplish this task, we utilize Whisper^[11], a large-scale weakly supervised pre-training model. Whisper has been developed specifically to facilitate robust speech recognition and feature extraction from audio data. By applying this cutting-edge technology, we can accurately analyze patients' breath sounds and extract relevant features indicative of respiratory conditions. This analysis ultimately results in the construction of an audio stream feature map, which complements the EMR feature map generated by Module 1.

By combining the insights gained from these two modules, the Rene architecture enables a holistic approach to patient diagnosis. This multi-modal fusion of structured medical record data and breath sound data allows for a more comprehensive understanding of patients' conditions, leading to more accurate diagnoses and, ultimately, improved patient care. The fusion of these data sources is achieved by leveraging advanced machine learning algorithms, which ensures that the architecture remains flexible and adaptable to accommodate new information and evolving diagnostic needs.

In this experiment, the Rene Trial Block shown in Figure 1B employ a ternary branch jump design that gradually contracts the receptive field on the left side while expanding the right. Incorporating residual connections within the central pathway aids in preserving the original features, thereby boosting the network's learning process and promoting stability and fluency.

The three-way branch design, which incorporates varying convolutional receptive fields and residual links, has numerous advantages. Firstly, it facilitates multi-scale feature learning. The decreasing receptive field on the left bypass captures detailed features, while the increasing receptive field on the right bypass grasps more abstract, broader features. This enables the model to understand and represent complex data patterns effectively. Secondly, the residual links improve gradient flow during backpropagation, mitigating the vanishing gradient problem commonly associated with deep neural networks. This makes training deeper networks more feasible. Thirdly, the model's robustness to scale variations is enhanced. With its ability to capture features at different scales, it can more effectively handle variations in input data scale. Lastly, this design offers computational efficiency. Each branch can be processed

independently, potentially enabling parallel processing.

Furthermore, by transforming audio features into two-dimensional feature maps, we enhance the model's perception of local attributes. Deep separable convolution, proficient in local feature extraction, empowers us to seize local patterns across various frequencies and time scales. This approach capitalizes on cross-channel and spatial correlations, contributing to a more in-depth understanding of lung audio data's internal structure.

We utilized the LightGBM^[12] algorithm, a gradient boosting framework that employs decision tree-based learning algorithms, to gauge the gain importance of EMR from the ICBHI 2017 Challenge Respiratory Sound Database^[13]. This model allows for a structured representation of the relationships between various features and facilitates a more in-depth understanding of the complex interconnections within EMR. This data-driven approach allowed us to pinpoint specific features that substantially enhance the model's accuracy when deployed for classification tasks.

In turn, as shown in Figure 1C, this analysis provided valuable insights into the significance of these key features in predicting respiratory diseases. By identifying the most influential factors, the interpretability of our model was greatly amplified. This not only increased transparency but also bolstered the model's predictive precision, thereby improving the clinical applicability of our findings.

For audio stream feature information, we applied a novel network architecture, Conformer^[14], which synergistically combines Convolutional Neural Networks (CNN)^[15] and Transformer^[16] models to extract rich and informative features from audio data. This hybrid approach capitalizes on the strengths of each model, resulting in a more robust and effective feature extraction process.

Specifically, CNN is employed for short-term temporal information extraction, enabling the network to capture local features in the audio more effectively. CNN is particularly adept at identifying and characterizing patterns within the data, making them well-suited for this task. By leveraging the power of CNN for short-term temporal analysis, we ensure that our network can accurately discern subtle variations in breath sound patterns, which are often indicative of respiratory conditions.

Meanwhile, Transformer and Bidirectional Gated Recurrent Units (Bi-GRU)^[17] models are utilized for long-term temporal information extraction, capturing global information within an extended range. These models are designed to handle sequential data more effectively, making them ideal for analyzing the broader patterns and trends that emerge over time in audio data. By incorporating both Transformer and Bi-GRU models into our network architecture, we enhance our ability to identify and interpret

significant long-term trends in patients' breath sounds.

By integrating these complementary models, our network architecture effectively captures both local and global features within audio data, resulting in a more accurate and comprehensive representation of patients' respiratory health. This innovative approach to feature extraction from audio stream data, when combined with the insights gleaned from structured EMR, allows for a more holistic and informed diagnosis of patients' conditions, ultimately leading to improved patient care and outcomes.

Physicians often rely on the combination of multiple disease symptoms to make accurate diagnoses. Drawing inspiration from this practice, we integrate features from both audio data and EMR to create a more comprehensive diagnostic model. As illustrated in Figure 1A, patient information features are extracted from two distinct modules, with each module outputting a probability prediction value for the same task. To fuse these predictions effectively, we employ the *Alpha* confidence level, which performs a probabilistic fusion of the two modes and generates the final prediction result for our architecture.

The Rene architecture primarily addresses four key tasks in respiratory system disease diagnosis, catering to the various stages of the diagnostic process:

1. **Respiratory Event Detection:** The architecture efficiently identifies and locates respiratory events in the audio data, which serve as vital indicators of potential respiratory issues. By leveraging the power of advanced machine learning algorithms, the Rene architecture can accurately detect and classify these events, providing crucial information for the subsequent stages of diagnosis.

2. **Breath Sound Recording Classification:** The architecture is designed to classify breath sound recordings based on their characteristics, such as wheezing, crackles, or normal breath sounds. This classification process allows physicians to efficiently analyze the audio data and identify patterns indicative of specific respiratory conditions.

3. **Respiratory Disease Diagnosis:** Building on the insights gained from the previous tasks, the Rene architecture employs the integrated features from both audio data and EMR to generate a comprehensive and accurate respiratory disease diagnosis. By combining the strengths of these two data sources, the architecture can provide a more nuanced and informed understanding of patients' conditions, ultimately leading to better patient care.

4. **Real-time Disease Monitoring Systems:** The Rene architecture is designed to facilitate the development of real-time disease monitoring systems, which can track patients' respiratory health and provide real-time feedback on their condition. By

continuously monitoring and analyzing breath sounds and other relevant data, these systems can enable physicians to identify and address potential issues more proactively, helping to prevent complications and improve overall patient outcomes.

In summary, the Rene architecture offers a multi-modal fusion approach to respiratory system disease diagnosis, harnessing the power of AI to analyze and integrate information from both audio data and EMR. By addressing key tasks within the diagnostic process and facilitating real-time monitoring systems, the architecture has the potential to significantly improve the accuracy of diagnoses and the quality of patient care.

Application of multi-modal advancements of Rene architecture on the ICBHI dataset

The publicly available ICBHI dataset comprises 928 lung sound recordings from 126 subjects, providing a valuable resource for our patient-level analysis. Our study focuses on the predictive accuracy of classifying eight distinct diseases using this audio data. The dataset is enriched with supplementary annotation files that supply vital metadata such as subject age, gender, and Body Mass Index (BMI), along with annotations for each respiratory cycle, specifying the presence or absence of crackles and wheezes. Furthermore, each recording in the ICBHI dataset is linked to the patient's disease condition, which is organized into three primary categories: chronic diseases (e.g., Chronic Obstructive Pulmonary Disease, Bronchiectasis, and Asthma), non-chronic diseases (e.g., upper and lower respiratory tract infections, pneumonia, and bronchiolitis), and a healthy group. This comprehensive dataset enables an in-depth investigation and understanding of disease classification, paving the way for potential advances in diagnosis and treatment.

In pursuit of the overarching goal of automating lung disease analysis and providing instant predictions for pulmonary clinicians, we employed a macroscopic approach emphasizing overall model predictability. To ensure robust predictions, we consolidated lung sound recordings from individual patients and rigorously validated the formatting of the data.

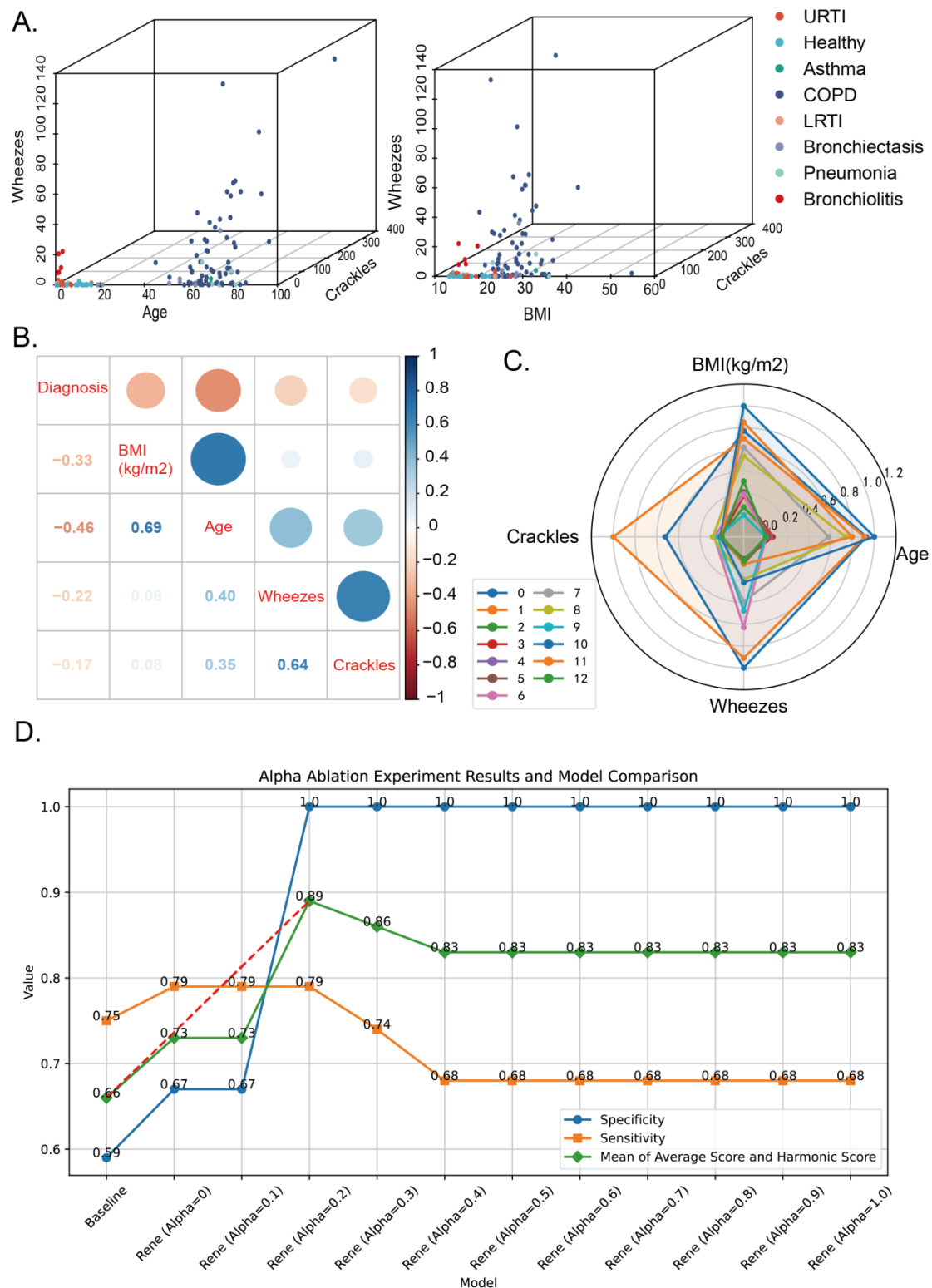


Fig2. Results of Rene architecture on ICBHI dataset. (A) Visualization of principal component features of electronic medical records in a 3-dimensional space. (B) Correlation analysis between disease diagnosis and primary feature dimensions. (C) Comparison of the four primary analysis characteristics' differences in each patient group using unsupervised clustering. (D) Ablation experiments for the confidence α on the ICBHI dataset, with comparison to the baseline.

After addressing missing values in the patient information, we transformed the eight lung disease categories (Asthma, Bronchiectasis, Bronchiolitis, Bronchitis, COPD, Healthy, LRTI, Pneumonia, URTI) from the ICBHI database into numerical labels using LabelEncoder^[18]. To examine the correlation between different numerical feature variables and disease classifications, we employed the Pearson correlation coefficient^[19]. The resulting coefficient matrix is visualized as a heatmap in Figure 2B. The Pearson correlation coefficient is calculated using the following formula:

$$\rho = \frac{Conv(X,Y)}{\sigma_X\sigma_Y} \quad (1)$$

The correlation coefficient ρ is calculated as the covariance $Conv(X,Y)$ between two variables divided by the product of their respective standard deviations $\sigma_X\sigma_Y$.

The correlation heatmap offers insights into the relationships between variables, revealing a significant correlation between BMI and age as well as a strong association between crackles and wheezes within patients' respiratory cycles. The numerical labels of lung diseases in the ICBHI database display varying degrees of correlation with numerical feature variables, with age, BMI, wheezes, and crackles ranking from highest to lowest in terms of correlation strength with disease diagnoses. Analyzing the correlation coefficient matrix provides valuable information on linear dependencies among variables, which is crucial for data preprocessing, feature engineering, and subsequent modeling efforts.

To ensure feature independence and minimize the impact of correlated fields on clustering results, it is common practice to exclude highly correlated variables before implementing unsupervised clustering techniques. In this experiment, we selected age and wheezes as numerical feature variables for K-means clustering, considering their significant correlations with lung disease diagnoses. This approach enhances the reliability and accuracy of our analysis in understanding and categorizing lung diseases.

Our study utilized 3D data visualization to extract critical features from medical records, a technique that reduces noise, standardizes features, and enhances model accuracy. We calculated the total number of crackles and wheezes within each respiratory cycle for every patient, denoting them as "Crackles" and "Wheezes," respectively. Using Age, Body Mass Index(BMI), Crackles, and Wheezes as coordinate axes and Diagnosis as the color label, we visualized the data distribution in a 3D interactive plot. This innovative approach offers valuable insights into the identification and understanding of lung diseases, potentially revolutionizing diagnosis and treatment strategies for clinicians.

The results reveal a highly imbalanced distribution of the original data across

various diagnoses. The population with Chronic Obstructive Pulmonary Disease (COPD) has the largest representation, and its distribution covers a wide range of values in the 3D space. This visualization offers valuable insights into the data distribution while emphasizing the significant class imbalance present in the original dataset. Figure 2A illustrates the resulting 3D data distribution, providing a clearer understanding of the relationships between lung diseases and their respective audio features.

The visual representation shows that "Healthy" individuals primarily exhibit data points concentrated near the axes within the crackles and wheezes dimensions. In contrast, patients diagnosed with "Bronchiolitis" predominantly lean towards wheezes. Similar patterns can be observed for other lung diseases. The interactive 3D plot allows for the exploration of individual patient profiles and the identification of variations among different cases. This, in turn, enables subsequent statistical analyses and deepens our understanding of the data, contributing to a more comprehensive assessment of lung disease classification and potential treatment strategies.

The Silhouette Coefficient is a method for evaluating the effectiveness of clustering. It was initially proposed by Peter J. Rousseeuw in 1986. The Silhouette Coefficient combines the concepts of cohesion and separation in clustering to assess its performance. It calculates the silhouette coefficient for each sample, which represents the degree of difference between the distance of the sample to its own cluster and the distance to the nearest neighboring cluster. The formula for calculating the silhouette coefficient is as follows:

$$S(i) = \frac{b(i) - a(i)}{\max\{a(i), b(i)\}} \quad (2)$$

Whereas $a(i)$ represents the cohesion of a sample point, it is calculated as follows:

$$a(i) = \frac{1}{n-1} \sum_{j \neq i}^n \text{distance}(i, j) \quad (3)$$

Where j represents other sample points within the same cluster as sample i , and distance denotes the distance between i and j . Therefore, $a(i)$ becomes smaller as the cluster becomes more tightly knit. The calculation of $b(i)$ is similar to $a(i)$, except that it involves iterating through other clusters to obtain multiple values. The minimum value from these values in $b(i)$ is selected as the final result. Consequently, the original $S(i)$ is transformed into the following calculation:

$$S(i) = \begin{cases} 1 - \frac{a(i)}{b(i)} & a(i) < b(i) \\ 0 & a(i) = b(i) \\ \frac{b(i)}{a(i)} - 1 & a(i) > b(i) \end{cases} \quad (4)$$

From the above equation, we can observe that when $a(i)$ is less than $b(i)$, indicating that the intra-cluster distance is smaller than the inter-cluster distance, the clustering result is tight in shape. In such cases, the value of S tends to approach 1, signifying a more pronounced silhouette. Conversely, when $a(i)$ is greater than $b(i)$, indicating that the intra-cluster distance is larger than the inter-cluster distance, it suggests that the clustering result is rather loose. Consequently, the value of $S(i)$ tends to approach -1, implying a poorer clustering performance. The value of $S(i)$ falls within the range of -1 to 1, with larger values indicating better clustering results^[20].

Cluster analysis groups data based on feature similarities, strengthening the correlation between samples and facilitating improved learning by deep learning models. We employed unsupervised K-means clustering on audio data from pneumonia patients and determined the optimal value of K (K=13, Silhouette Coefficient=0.85) corresponding to the maximum silhouette coefficient. Subsequently, we calculated the mean of numerical features and the mode of categorical features within each cluster group. Table 2 presents the grouping characteristics of K-means clustering.

Each cluster group captures patients with specific similarities, enabling doctors to gain a better understanding of their conditions and provide tailored treatments for different groups. This ultimately enhances the effectiveness of diagnosis and treatment, contributing to more personalized and targeted healthcare for patients with lung diseases.

Table 1. Grouping Characteristics of K-means Clustering

Clusters	Coun ts	Percen tage	Age	BMI (kg/m2)	Crack les	Wheez es	Se x	Diagnosis
0	48	38%	69	27.32	28.83	19.85	M	COPD
1	16	13%	68	26.29	55.31	18.06	F	COPD
2	13	10%	6	17.07	0.77	0	M	Healthy
3	13	10%	6	18.59	0.54	0.23	F	Healthy
4	8	6%	4	19.03	1.88	0.38	F	URTI

5	6	5%	3	19.12	1	0.83	M	URTI
6	4	3%	2	18.82	4	12.5	M	Bronchiolitis
7	5	4%	44	25.11	4.4	7.8	F	Bronchiectasis
8	4	3%	55	23.94	4.75	3.75	M	Pneumonia
9	2	2%	2	16.01	2	9.5	F	Bronchiolitis
10	3	2%	74	30.67	0.67	4.33	F	Pneumonia
11	2	2%	60	28.49	0	1	M	Bronchiectasis
12	2	2%	2	20.55	0	0.5	M	LRTI

By combining the clustering analysis results from Table 1 and plotting the feature comparison radar chart (Figure 2C) on the main principal dimensions (Age, BMI, Crackles, and Wheezes), we can visually discern the distinct differences between various groups. The data distribution reveals that the highest proportions correspond to Class 0 and Class 1, both associated with COPD symptoms. These classes exhibit older age, higher BMI indices, and increased frequencies of coughing and wheezing during the respiratory cycle. In contrast, the healthy populations in Class 2 and Class 3 are characterized by younger age, moderate body mass, occasional mild crackles during the respiratory cycle, but no wheezing symptoms. We applied similar analysis methods to examine the characteristics of the remaining minority groups, contributing to a comprehensive understanding of the diverse lung disease categories and their respective features.

The aforementioned process of 3D visualization and clustering analysis of patient information is used to perform patient data preprocessing, classification, and filtering. This enables us to extract pneumonia-related features from lung sound audio data and subsequently classify them into distinctive groups of disease types, thereby providing a comprehensive, standardized output for subsequent deep learning processing.

Figure 2A highlights the highly imbalanced sample distribution across various medical conditions in the original ICBHI dataset. COPD-associated samples dominate the majority of the sample space, while minority class samples are insufficient for effectively learning decision boundaries and avoiding overfitting during the learning process. To address this issue, we balance the sample distribution by oversampling minority class samples in medical records using the SMOTE algorithm^[21], ensuring a balanced distribution in the augmented dataset. SMOTE's working mechanism involves randomly selecting a minority class sample, identifying its k (usually $k=5$) nearest neighbors, and subsequently creating a synthetic sample between two points in the

feature space. Our study employs LightGBM, a distributed and efficient gradient boosting framework that utilizes decision trees based on learning algorithms. Notably, LightGBM demonstrates faster fitting speeds compared to Xgboost^[22] on various datasets^[23], making it particularly advantageous for deploying real-time lung sound detection models on edge AI devices.

Most machine learning algorithms have inherent limitations in constructing individual models. The more information we gather before making a decision, the greater the likelihood of making the correct decision^[24]. Therefore, our natural inclination is to integrate predictions from multiple models to overcome the shortcomings of individual models and provide a comprehensive final decision. Given that clinical diagnosis requires the integration of patient medical records and multi-modal information such as audio auscultation, we choose to use confidence to combine the probability predictions from the output of Rene Trial Block and the classification probability values from LightGBM. The calculation method is as follows:

$$Output(p_t) = Alpha * Rene(p_t) + (1 - Alpha) * LightGBM(p_t) \quad (5)$$

Where p_t represents the estimated probability of the numerical labels for each disease category. $Alpha$ is a hyperparameter that guides the prediction results to be more biased towards either audio features or medical records. To showcase the effectiveness of the multi-modal fusion Rene architecture, we conducted an ablation study to investigate the impact of the $Alpha$ value, which is chosen from the range of 0 to 1 with a step size of 0.1.

To evaluate and compare the performance of our models with state-of-the-art systems, we employ sensitivity (Se.), specificity (Sp.), and ICBHI scores (average score (AS) and harmonic score (HS)) as assessment metrics, as detailed in^{[25], [26], [27]}. Figure 2D presents the models' performance on the test set at different confidence levels (baseline reference^[28]), with results rounded to two decimal places.

As $Alpha$ increases, the model leans more towards the output of the audio feature extraction network, leading to a progressive improvement in specificity (Spec.), indicating enhanced accuracy in detecting healthy subjects. However, the model's sensitivity (Sen.) initially increases and then decreases, signifying a rise in the misdiagnosis rate for patients with respiratory diseases. The Rene architecture at $Alpha=0.2$ demonstrates the best performance on the ICBHI test set, with a 23% improvement in the mean of average score (AS) and harmonic score (HS) compared to the baseline, showcasing its competitive advantage.

Micro-level classification models offer high interpretability by providing the probability of each respiratory event belonging to a specific category based on external

sounds. However, when evaluating decisions for each respiratory cycle of a patient, we observe that not all cycles exhibit crackles and wheezes. In other words, even if certain respiratory cycles lack crackles and wheezes, we cannot confidently consider the subject as healthy. This is because the majority of respiratory cycles for many subjects, including patients, are normal. Consequently, we cannot rely solely on the presence of crackles and wheezes within respiratory cycles to determine a patient's condition. This limitation is one reason why we consider the confidence level *Alpha* to combine multi-modal analysis for respiratory diseases. Furthermore, it highlights the importance of observing trends and incorporating additional information to enhance diagnostic accuracy and understanding of patients' conditions.

Verification of the backbone of the Rene architecture on the SPRSound dataset

In this study, we evaluated the performance of the backbone of our proposed Rene architecture for lung sound detection using the open-source respiratory sound databases: SPRSound. SPRSound, developed by Shanghai Jiao Tong University, is the first open-source pediatric respiratory sound database, containing 2,683 recordings and 9,089 events from 292 participants^[29]. The creation process involved custom sound annotation software for editing and quality assessments, with 11 experienced pediatric doctors establishing the gold standard reference. On the other hand, ICBHI is a large respiratory dataset with 920 samples from 126 patients, totaling 5.5 hours of audio and featuring 8,877 annotated crackles and 1,898 annotated wheezes. Evaluating our proposed Rene model on these two lung sound datasets further demonstrated its accuracy and generalization across different age groups and ethnicities.

Furthermore, our experiment focuses on respiratory sound from three distinct dimensions: events, recordings, and patients. Lung sounds are categorized based on various characteristics, including duration and pitch^[30]. Notably, the unclassified category can be further subdivided into continuous and discontinuous events, based on their continuity/duration. Given that the SPRSound database only provides label annotations at the event and recording levels, our evaluation primarily assesses the detection effectiveness of the Rene architecture at the respiratory event and audio recording levels. This database selection is akin to conducting ablation experiments on patient medical records, specifically evaluating the efficacy of the backbone network in the Rene architecture solely on the respiratory audio database.

In contrast, the ICBHI dataset offers comprehensive annotations encompassing

detailed patient information including: binary annotations indicating the presence or absence of crackles and wheezes within each respiratory cycle in the audio recordings, patient demographic data such as age, height, and weight. Thus, we utilize the full Rene architecture combined with multi-modal integration to investigate respiratory disease prediction at the patient level, capitalizing on the extensive annotations available in the ICBHI dataset.

The SPRSound training set comprises 1,949 audio recordings and 6,656 respiratory sound events from 251 participants. The test set contains 734 audio recordings and 2,433 respiratory sound events, featuring both the same participants from the training set and additional individuals. Crucially, respiratory sounds are categorized into normal and adventitious sounds. Adventitious sounds can be further classified based on their duration as continuous adventitious sounds (CAS)—including Rhonchi, Wheeze, and Stridor—or discontinuous adventitious sounds (DAS), such as Coarse Crackle and Fine Crackle^[31]. Given the SPRSound database, the developers proposed two levels of classification tasks to address the dataset's specific characteristics.

Task 1 (Respiratory Sound Classification at the Event Level)

Task 1-1: This binary classification task aims to categorize respiratory sound events as either "Normal" or "Adventitious." The goal is to distinguish normal respiratory sounds from those exhibiting adventitious characteristics.

Task 1-2: This multi-class classification task seeks to categorize respiratory sound events into seven classes, including "Normal," "Rhonchi," "Wheeze," "Stridor," "Coarse Crackle," "Fine Crackle," and "Wheeze & Crackle." The objective is to differentiate between normal respiratory sounds and various types of adventitious sounds, such as specific categories of crackles, wheezes, and other abnormal respiratory sounds.

Task 2 (Respiratory Sound Classification at the Recording Level)

Task 2-1: This ternary classification task aims to categorize respiratory sound recordings as "Normal," "Adventitious," or "Poor Quality." The goal is to differentiate between normal recordings, those with adventitious sounds, and poor-quality recordings that may impact the analysis's accuracy.

Task 2-2: This multi-class classification task seeks to categorize respiratory sound recordings into five classes, including "Normal," "Continuous Adventitious Sounds (CAS)," "Discontinuous Adventitious Sounds (DAS)," "CAS & DAS," or "Poor Quality." The objective is to classify recordings based on the presence of normal sounds, continuous or discontinuous adventitious sounds, and poor-quality recordings with

artifacts or other issues affecting the analysis.

Sensitivity (SE) and Specificity (SP) are widely used in the medical field to evaluate the accuracy of diagnostic tests^[32]. In assessing lung sound detection models, we adopt evaluation criteria from the IEEE BioCAS 2022 Respiratory Sound Classification Challenge^[33]. The evaluation metrics for each task encompass Sensitivity (SE), Specificity (SP), Average Score (AS), Harmonic Score (HS), and Final Score, defined as follows:

$$SE = \frac{\sum P_i}{\sum N_i} \quad (6)$$

$$SP = \frac{P_N}{N_N} \quad (7)$$

$$AS = \frac{SE+SP}{2} \quad (8)$$

$$HS = \frac{2*SE*SP}{SE+SP} \quad (9)$$

In this paper, P_i and P_N represent the number of accurately classified samples for adventitious class i and Normal class, respectively. Conversely, N_i and N_N denote the total number of samples for adventitious class i and Normal class individually. These definitions will be crucial for our analysis and discussion. The final score for each task is the mean of the Average Score (AS) and Harmonic Score (HS). This provides a concise and balanced evaluation of the model's performance.

$$Score = \frac{AS + HS}{2} \quad (10)$$

In this experiment, we employ a Mel filter bank with a cutoff frequency range of 50 Hz to 2.5 kHz for respiratory sounds, chosen to suppress background noise from equipment aging or operational errors, leaving only clean respiratory sound signals. Upon analyzing the data, we observed a significant imbalance in the SPRSound dataset, with the "Normal" class vastly outnumbering other classes at both the respiratory event and audio recording levels. Drawing inspiration from Li Jun et al.^[34], we implemented two methods to address this severe class imbalance issue: WeightedRandomSampler^[35] and Focal Loss^[36].

Due to hardware limitations, such as the size of the CUDA memory, it may not be feasible to load a large amount of data into the network for training all at once. Therefore, it becomes necessary to read the data in batches. When encountering the problem of imbalanced sample data, WeightedRandomSampler (WRS) can be employed to balance the samples within each batch based on their respective weights,

thereby improving the performance of the model.

Additionally, when dealing with imbalanced datasets, WRS helps adjust the sampling probabilities for each sample, ensuring that samples from different classes are represented approximately equally within each batch. By assigning weights to each sample, we determine the appropriate weight for each class and assign it to the corresponding samples. This approach allows better handling of minority class samples and enables the model to effectively learn from balanced sample sets.

Focal Loss is a variant of Cross Entropy Loss (CE). When an overwhelming number of easily distinguishable negative samples dominate the CE loss, focus on positive samples is diminished. Focal Loss addresses this issue by introducing a dynamic scaling factor that reduces the weight of easily distinguishable samples during training. This approach allows the model to quickly shift its focus to more challenging samples, enabling them to dominate the gradient during training. The formula for Focal Loss is as follows:

$$F_l(p_t) = -(1 - p_t)^\gamma \log(p_t) \quad (11)$$

The modulation factor $(1 - p_t)^\gamma$ is utilized in Focal Loss to reduce the contribution of easily classified samples. As p_t increases, indicating that a sample is easier to distinguish, the modulation factor decreases. The parameter γ controls the rate at which the loss is reduced for easily classified samples and can take values in the range of $[0, 5]$. When γ is set to 0, the Focal Loss reduces to the original Cross Entropy Loss. In the original Focal Loss paper, the authors found that $\gamma = 2$ yielded the best experimental results. With $\gamma = 2$, the loss for an example with $p_t = 0.9$ is reduced by a factor of 100 compared to the Cross Entropy Loss, and when $p_t \approx 0.968$, the loss is reduced by a factor of 1000. Inspired by these findings, we adopt $\gamma = 2$ as the default parameter for training the Rene architecture with Focal Loss in this study.

We trained the model using an NVIDIA Tesla A100 GPU on an Ubuntu 22.04 LTS platform. During the training process, we set the default batch size to 16, the number of epochs to 60, and the initial learning rate to 0.000001. The learning rate exponentially decayed by a factor of 0.1 every 2k steps, ensuring better stability in the later stages of training.

The mel frequency cepstral coefficient (MFCC)^[37] method effectively simulates the response of the human auditory system and provides features with excellent discrimination and low correlation in various patient combinations, inter-patient comparisons, and overall classification analyses. The MFCC method, when combined with the Naive Bayes (NB)^[38] classifier, demonstrated superior performance in tasks 1-1 and 1-2 compared to other machine learning algorithms. This underscores the

effectiveness of low correlation MFCC features in achieving robust classification results using the NB classifier. Furthermore, the MFCC method paired with the support vector machine (SVM)^[39] classifier also exhibited high classification performance in tasks 2-1 and 2-2.

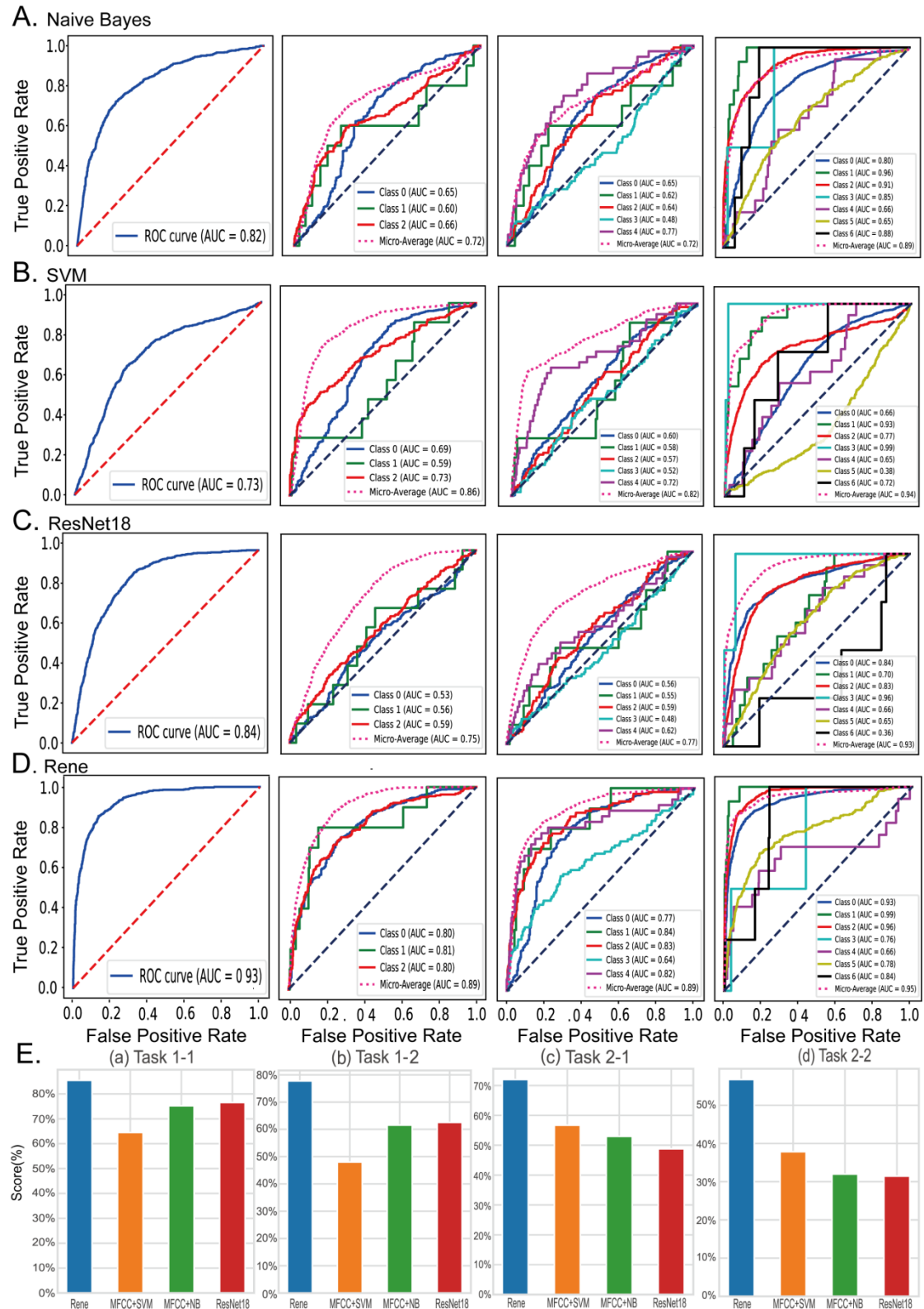


Fig3. Performance Comparison of Various Models on the SPRSound Database.

(A) (B) (C) (D). We conducted a detailed comparison of the performance of different models on the SPRSound database, encompassing Naive Bayes, SVM, ResNet18, and our proposed Rene model. The analysis comprises four distinct classification tasks, with the results displayed in panels (A), (B), (C), and (D). The panels illustrate the Area Under the Curve (AUC) and Receiver Operating Characteristic (ROC) scores for each model, providing a comprehensive assessment of their performance across the SPRSound database classification tasks. **(E).** Panel E offers a direct comparison of Rene's performance against the other models. The score enables an unbiased assessment of the relative performance of our proposed Rene architecture, highlighting its potential advantages in the realm of lung sound detection and respiratory disease diagnosis.

We utilized the best-performing machine learning methods for each task, as provided by the SPRSound database developers, to serve as baseline models. These baselines achieved scores of 75.22%, 61.57%, 56.71%, and 37.84% in the four classification challenges at the event and recording levels, respectively^[29]. In comparison, our Rene architecture demonstrated a marked improvement, attaining the highest scores of 85.46%, 77.72%, 72.00%, and 56.74% in the four tasks, respectively. When compared to the baseline models, our proposed Rene architecture improved performance by 10.24%, 16.15%, 15.29%, and 18.90% in the corresponding tasks. These results not only highlight the significant advantages of our proposed architecture for lung sound detection tasks but also underscore the potential for enhancing diagnostic accuracy in respiratory system disease diagnosis.

To further compare the performance of our Rene model with state-of-the-art lung sound detection models, we reproduced the top-performing model (with ResNet18 as the backbone) from the IEEE BioCAS 2022 Respiratory Sound Classification Challenge. We then compared its scores on the SPRSound database tasks with those of our Rene model to gain a deeper understanding of the relative performance of our proposed architecture. The results of this comparison are depicted in a bar graph in Figure 2E, which clearly demonstrates the competitive performance of our Rene architecture in lung sound detection tasks.

The increased performance of the Rene architecture can be attributed to its multi-modal fusion approach, which integrates information from both audio data and electronic medical records. This combination of data sources enables a more comprehensive understanding of patients' conditions, which in turn leads to better diagnostic performance. Furthermore, the innovative network architecture and ternary branch jump design, which effectively facilitate multi-scale feature learning, resulting in a more accurate representation of patients' respiratory health.

In conclusion, the improved performance of the Rene architecture highlights the value of employing advanced model architecture design and multi-modal fusion approaches in respiratory system disease diagnosis. By integrating information from different data sources and leveraging state-of-the-art AI models, the Rene architecture has the potential to significantly enhance the accuracy of diagnoses and ultimately improve patient care and outcomes.

DISCUSSION

In this study, we present a deep learning approach for analyzing lung sound data and introduce a novel multi-modal architecture called Rene. The architecture employs the Whisper pre-trained model to extract decoded audio features, which are then re-encoded and re-decoded through the Conformer and BiGRU networks. After 3D data visualization and clustering analysis of patient records, we fuse the predicted disease probabilities from the Rene Trial Block with the patient feature classification probabilities computed by LightGBM, using the confidence level *Alpha*.

Compared to the baseline model of SPRSound database, the proposed Rene architecture achieves performance improvements of 10.24%, 16.15%, 15.29%, and 18.90% in four tasks, respectively. In patient disease prediction tests conducted on the ICBHI database, the mean of average score and harmonic score of the proposed model improved by 23%, compared to the baseline model. The algorithm effectively classifies lung diseases and healthy populations with high accuracy while minimizing the risk of cross-infection.

We also propose a real-time disease diagnosis system based on Rene architecture for analyzing respiratory audio data. The detail of this system is included in the Methods section. This system features a dual-thread design that enables simultaneous microphone recording and real-time dynamic decoding through compressed model parameters. This edge-AI art facilitates rapid response disease diagnosis and can be implemented on wearable clinical detection devices, further advancing the development of edge AI in the realm of respiratory disease detection.

The proposed Rene architecture demonstrates promising performance in tasks such as respiratory sound discrimination and real-time diagnosis. We suggest three main directions for future work:

1. Integrating CT imaging data with the multi-modal Rene model for lung disease diagnosis: Current research primarily focuses on methods for lung sound data processing. Incorporating CT imaging data can offer more comprehensive lung

information, thereby improving diagnosis accuracy and reliability. Future work should explore effective multi-modal fusion methods and confidence-weighted integration of CT imaging data within the Rene model to enhance its utilization and generate reliable diagnostic results.

2. Simulating lung sound data using GAN^[40] models: Employing generative adversarial network (GAN) models can simulate and generate high-fidelity lung sound data, increasing the training dataset's size and diversity. This will improve the model's robustness and generalization ability, enabling it to adapt to a broader range of respiratory sound data. Combining GAN techniques with lung disease diagnosis models is crucial for enhancing model performance and reliability.

3. Synergistic adaptation with large language models (LLMs) such as GPT-4^[41] in downstream tasks: LLMs like GPT-4 represent breakthroughs in artificial intelligence, transitioning from weak to general AI. Extending Rene with LLMs in downstream tasks can further expand lung disease diagnosis application domains. As real-time respiratory sound data rapidly accumulates from precision medicine, training larger, deeper models becomes possible. Edge AI models can then acquire stronger semantic understanding and reasoning capabilities, enhancing their performance in more complex tasks, such as real-time clinical decision support. This synergistic evolution will foster greater breakthroughs and advancements in lung disease diagnosis.

In conclusion, integrating CT imaging data with the multi-modal Rene architecture, simulating lung sound generation using GAN models, and synergistically evolving with large models like GPT-4 are potential future extensions of our work. Investigating these directions will contribute to improving lung disease diagnosis models' performance, reliability, and application scope, driving progress in this field.

METHODS

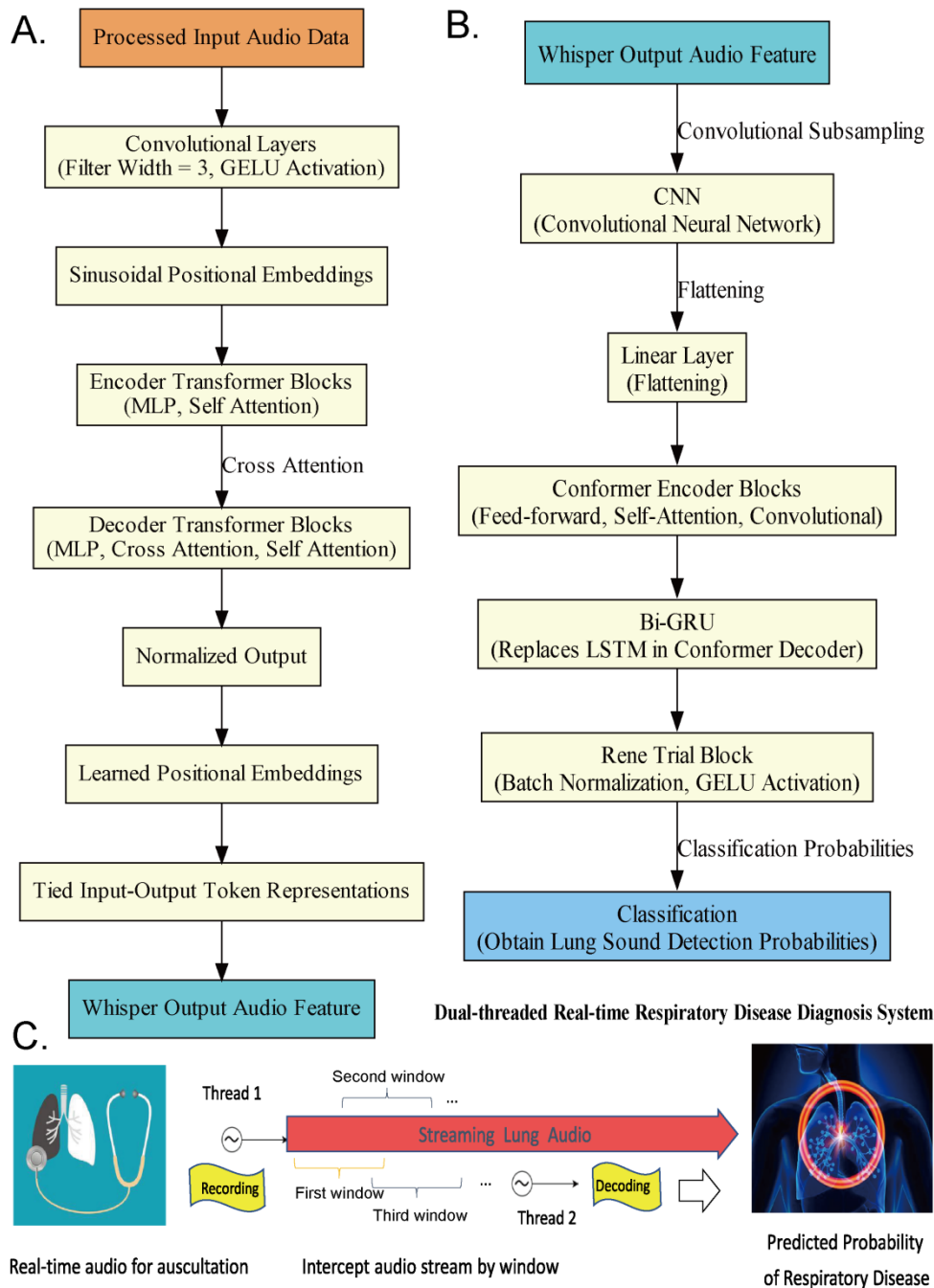


Fig4. The key parts in Rene architecture. (A) Robust Speech Recognition Based on Large-Scale Weak Supervision: Whisper's Network Architecture. The Rene architecture involves the use of Whisper, a large-scale weakly supervised pre-training model specifically designed for robust speech recognition and feature extraction from audio data. Whisper's network architecture effectively processes and analyzes patients' breath sounds, identifying meaningful patterns and features that can aid in the diagnostic process. **(B)** Conformer: Convolution-augmented Transformer for Speech Recognition. The Conformer is an advanced model that combines the strengths of Convolutional

Neural Networks (CNN) and Transformer models to facilitate more effective speech recognition. By incorporating convolutional layers into the Transformer architecture, the Conformer is capable of capturing both local and global patterns in audio data, resulting in a richer representation of patients' respiratory health and ultimately improving diagnostic accuracy. (C) Dual-Threaded Audio Recording and Real-Time Dynamic Decoding Output for Respiratory Disease Classification. The dual-threaded real-time respiratory disease diagnosis system, based on the Rene architecture, features an innovative approach to simultaneously processing audio recordings and dynamically decoding outputs for respiratory disease classification.

Detailed analysis of Rene architecture

To improve the accuracy and robustness of our model in analyzing pulmonary audio data, we employ several data preprocessing steps. First, the audio data is converted to numeric input and normalized and globally scaled to a range of -1 to 1, setting the pre-training dataset's mean to zero. Next, we use a 25-millisecond window with a 10-millisecond stride to compute the logarithmic mel-spectrogram representation using 80 channels.

The logarithmic mel-spectrogram offers several advantages, such as reducing audio data dimensionality, extracting discriminative and representative features, and enhancing the model's efficiency and precision. Notably, it also demonstrates favorable human perceptual attributes and resistance to interference, enabling better representation of lung sound data and potentially improved diagnostic capabilities for pulmonary diseases. The process of extracting logarithmic mel-spectrogram features from audio typically involves the following steps:

1. Preemphasis: Preemphasis is applied to the audio signal to boost high-frequency components. Let $x(n)$ represent the speech sample value at time n . The calculation of the pre-emphasized result $y[n]$ is as follows:

$$y[n] = x[n] - \alpha x[n - 1] \quad (12)$$

In this case, the preemphasis coefficient α is typically set to 0.97. The formula represents a first-order differencing operation, which can be interpreted as a high-pass filter.

2. Windowing: Each frame is subjected to windowing, commonly using a Hamming window. The formula for calculating the Hamming window is as follows, where N denotes the order:

$$w_{\text{ham}}(n) = \alpha - \beta \cdot \cos\left(\frac{2\pi n}{N-1}\right) \quad \alpha = 0.53836, \beta = 0.46164 \quad (13)$$

3. Fast Fourier Transform (FFT): After windowing each frame, a Fast Fourier Transform (FFT) is applied to obtain the frequency spectrum. The FFT principle

capitalizes on the symmetrical and periodic nature of signals to decompose the Fourier transform calculation into smaller subproblems. It employs a divide-and-conquer strategy by iteratively partitioning the signal into two sub-signals and computing them with rotation factors. This approach substantially diminishes computational complexity, rendering the FFT more efficient than direct Fourier transform calculation. The formula for the FFT calculation is as follows:

$$X(k) = \sum_{n=0}^{N-1} x[n] e^{-\frac{j2\pi kn}{N}} \quad (14)$$

In the equation, $X(k)$ represents the k -th frequency component of the frequency domain signal, $x(n)$ represents the sampled value of the time domain signal at discrete time point n , and N represents the length of the time domain signal.

4. Filtering with a set of Mel filters: After the FFT, the resulting signal is passed through a set of Mel filters to obtain the energy distribution in the Mel frequency scale. The conversion formulas between Mel scale and Hz are as follows:

$$\begin{cases} \text{mel} = 2595 \log_{10} \left(1 + \frac{\text{hz}}{700} \right) \\ \text{hz} = 700 \left(10^{\frac{\text{mel}}{2595}} - 1 \right) \end{cases} \quad (15)$$

5. Logarithm transformation of filtered energy: After filtering the signal, we logarithmically transform the energy values to obtain Mel Frequency Cepstral Coefficients (MFCC). This step compresses the signal's dynamic range and emphasizes crucial features. We generate the logarithmic mel-spectrogram from the audio signal and obtain the resulting MFCC from the mel-spectrogram to serve as input for the pre-trained lung sound analysis model. The logarithmic mel-spectrogram offers a compact representation of the audio signal, capturing essential frequency and temporal information for further analysis and modeling.

We employed the Whisper speech recognition model, which follows a Transformer encoder-decoder architecture. The encoder takes processed input data and applies two convolutional layers with a filter width of three and the GELU activation function^[42]. It then adds sinusoidal positional embeddings to the main output, which are carried over to the encoder Transformer blocks. Pre-activation residual blocks^[43] maintain the model's stability and efficiency, and the last layer of the encoder output is normalized. In the whisper decoder, the model uses learned positional embeddings and tied input-output token representations^[44]. Overall, the Whisper model aims to leverage the strengths of these components for accurate and efficient speech feature processing. Figure 4A illustrates the specific structure.

The Transformer model excels at capturing global interactions, while the CNN is

particularly adept at utilizing local features. In our proposed Rene architecture, we incorporate a structure known as Conformer into the backbone network, enabling it to model the semantic audio features extracted from Whisper decoding. This melding of the CNN and Transformer facilitates simultaneous consideration of both local and global dependencies within the audio features. Initially, the audio encoder component of the Conformer applies a convolutional subsampling layer to analyze the audio features generated by the Whisper module. Following the flattening of the input data using a linear layer, multiple Conformer Blocks are employed for encoding purposes. Each of these blocks comprises two feed-forward layers featuring half-step residual connections, interspersed with multi-head self-attention and convolutional modules. Through the creation of this highly integrated architecture, we effectively harness the strengths of various models to enhance the performance of the Automatic Lung Sound Recognition (ALSR) task.

In the original Conformer model, a single LSTM^[45] layer served as the decoder. However, a study by Fu-Shun Hsu et al. on the HF_Lung_V1 open-source lung sound database^[46] revealed that Bi-GRU consistently outperformed LSTM in various detection tasks, as evidenced by significantly higher F1-scores. Consequently, this paper replaces the decoder layer following the Conformer module with Bi-GRU. RNN networks are characterized by each node receiving the output (i.e., hidden state) of the previous node as input. Accordingly, the information contained in the last node of the decoder is fed into Rene Trial Block. The Rene Trial Block processes the information to obtain classification probabilities for lung sound detection.

In medical image recognition, widely-used CNNs and other models typically treat pixel data as a single input modality, neglecting to incorporate contextual clinical information. This limitation can hinder their clinical application and translation. For instance, in a patient with fever and elevated white blood cell count, a chest X-ray examination may accurately indicate pneumonia. However, for patients lacking supporting clinical features and laboratory results, similar radiographic findings could represent alternative etiologies, such as atelectasis, pulmonary edema, or even lung cancer^[47].

Similar examples can be found in the medical audio analysis domain, where clinical contextual information—typically derived from structured electronic health records data—is vital for achieving accurate and reliable results. The model architecture designed in this study employs a multi-modal approach, training separate models using features from different modalities, such as electronic medical records and audio data. The output probabilities of these multiple models are fused using confidence weighting to make the final decision. The selection of confidence weighting is often empirical and

depends on the application scenario and input modalities.

Owing to the limited medical records in most medical audio databases, which provide annotations only at the level of audio and respiratory events, data related to patient privacy and information, such as age, height, and weight index, are absent. Consequently, we utilize the Rene architecture backbone (shown in the lower panel of Figure 1A) exclusively on the available audio data. In databases with complete patient information, records are typically structured data. Ravid et al. discovered that integrating tree-based model with deep learning models yielded optimal results for structured feature datasets^[48]. The ultimate goal of this study is to deploy the model on edge AI devices, creating a real-time lung sound discrimination system. Consequently, there is a high demand for the model's real-time diagnostic speed. LightGBM significantly outperforms XGBoost in computational speed and memory consumption. As a result, we use LightGBM in our Rene architecture to process EMR. The prediction probability output of the LightGBM model is then fused with Rene Trial Block for the final lung sound classification task discrimination.

In this study, we explored various combinations of model hyperparameters, such as network depth, model dimension, and the number of attention heads, to select the best-performing models within the constraints of model parameter size. Ultimately, we finalized two models: Rene (S), a small model with 79M parameters, and Rene (L), a large model with 1752M parameters. In our experiments, Rene (L) was utilized for model performance validation, while Rene (S) was deployed on intelligent terminal devices. Table 2 outlines the architectural hyperparameters of these models.

Table 2. Hyperparameter of Rene (S) and Rene (L)

Model	Rene(S)	Rene(L)
Whisper Layers	4	32
Whisper Output Dim	384	1280
Whisper Attention Heads	6	20
Conformer Encoder Layers	16	17
Conformer Encoder Dim	256	512
Conformer Attention Heads	4	8
BiGRU Decoder Dim	512	512

Real-time auscultation system

Presently, artificial intelligence (AI) computations predominantly occur in data centers or the "cloud." However, cloud-centric architectures may not be ideal for addressing information security concerns and power consumption challenges in product design. We advocate for the development of edge-based AI for diagnosing respiratory system diseases using lung sound data, wherein algorithm models are deployed on intelligent terminals. This approach offers several advantages. First, it facilitates real-time decision-making by reducing network latency and conserving bandwidth. Second, it significantly enhances data security by eliminating the need for data transmission, which is essential for safeguarding patient privacy.

To optimize the computational efficiency of edge AI devices, we have successfully compressed the parameter size of the Rene model while maintaining its prediction accuracy without a significant decrease. The smaller, distilled model allows for rapid and precise real-time identification of respiratory sound pathologies in clinical environments. We strongly recommend implementing the streamlined Rene (S) architecture to enhance diagnostic capabilities.

The complexity of data in terminal systems for diverse populations often renders a single database ineffective in capturing all common lung sound features. To overcome this, we combined the International Conference on Biomedical and Health Informatics (ICBHI) database and the King Abdulaziz University Hospital (KAUH) database^[49], resulting in 1,256 respiratory sound recordings from 238 participants for model training. The ICBHI database offers event-level annotations for respiratory sounds, comprising 3,642 Normal, 1,864 Crackles, 886 Wheezes, and 506 Crackles & Wheezes. Meanwhile, the KAUH database provides recording-level annotations, including 35 Normal, 23 Crepitus, 41 Wheeze, 8 Crackle, 1 Bronchial, 2 Wheeze & Crackle, and 2 Bronchial & Crackle. The fusion databases encompass detailed patient information, such as records of 11 common diseases (e.g., Asthma, Heart Failure, Pneumonia, Bronchitis, Bronchiectasis, Bronchiolitis, Pleural Effusion, Lung Fibrosis, Lower Respiratory Tract Infection (LRTI), Upper Respiratory Tract Infections (URTI), and Chronic Obstructive Pulmonary Disease (COPD)), along with respiratory sound data from a total of 15 diseases. By combining these databases, our data ensures adequate generalization and adaptation for real-world scenarios.

In this experiment, we implemented a real-time respiratory sound flow diagnosis system on edge AI devices using a dual-thread design. One thread handles microphone audio recording (Recording), while the other manages real-time dynamic decoding

(Decoding on-the-fly). The stethoscope connected to the terminal's microphone processes data in 10ms audio data point units and feeds it into a 60-minute ring buffer. Every 10 seconds, a Mel feature calculation window extracts streaming audio data, which is then input into the model for real-time probability inference of disease classification, as depicted in Figure 4C.

The dual-threaded system comprises two primary components: 1. Audio Recording: The system efficiently captures and processes patients' breath sounds, utilizing cutting-edge models like Whisper and Conformer to effectively extract relevant features from the audio data. By accurately analyzing these features, the system can identify patterns indicative of specific respiratory conditions, such as wheezing, crackles, or normal breath sounds. 2. Real-Time Dynamic Decoding Output: Alongside the audio recording component, the system dynamically decodes the output patterns for respiratory disease classification in real-time.

To facilitate the deployment of this model on wearable respiratory sound detection terminal devices, we have open-sourced the code and model for the Dual-Thread Auscultation Stream Real-time Output System at <https://github.com/zpforlove/Rene>. This effort aims to advance the application of edge AI in diagnosing respiratory system diseases.

The Dual-Thread Auscultation Stream's automatic identification solution for real-time disease probability output offers several advantages over traditional auscultation methods:

1. Objectivity: Traditional auscultation relies on medical professionals' subjective analysis of audio signals, which can be influenced by personal biases and equipment accuracy. The automatic identification solution eliminates human errors, enhancing diagnostic accuracy and consistency.

2. Real-time capability: This solution delivers real-time disease probability outputs based on auscultation stream audio data, making it ideal for rapid decision-making scenarios, such as emergency departments and outpatient clinics.

3. Accuracy: Combining the Rene architecture with the real-time diagnostic solution for auscultation stream audio accurately predicts disease probabilities, assisting medical professionals in providing precise diagnostic results and improving respiratory system disease diagnosis.

4. Scalability: The solution's applicability extends beyond auscultation stream audio data to other non-contact monitoring scenarios, such as daily heart rate and respiratory monitoring, showcasing its scalability and adaptability.

5. Security: Deployment on edge AI devices eliminates the need for data transmission, saving bandwidth and significantly enhancing data security while protecting patient privacy.

In conclusion, the Dual-Thread Auscultation Stream's automatic identification solution for real-time disease probability output, based on the Rene model, holds promising prospects and practicality. It effectively improves the accuracy and efficiency of medical diagnosis. By concurrently processing audio recordings and dynamically decoding outputs, the dual-threaded real-time respiratory disease diagnosis system enhances the efficiency of the diagnostic process, enabling healthcare professionals to make more informed decisions and provide better patient care. Furthermore, the system's real-time capabilities facilitate continuous monitoring of patients' respiratory health, allowing for proactive identification and management of potential issues, ultimately contributing to improved patient outcomes.

REFERENCES

- [1] Morillo DS, León Jiménez A, Moreno SA. Computer-aided diagnosis of pneumonia in patients with chronic obstructive pulmonary disease. *J Am Med Inform Assoc.* 2013 Jun;20(e1):e111-7. doi: 10.1136/amiajnl-2012-001171. Epub 2013 Feb 8. PMID: 23396513; PMCID: PMC3715359.
- [2] Porhomayon, J., Papadakos, P., Singh, A., Nader, N. D., & El-Solh, A. A. (2012). The history of respiratory auscultation. *American Journal of the Medical Sciences*, 344(4), 308-311.
- [3] Bates, B. (2017). *A guide to physical examination and history taking.* Wolters Kluwer Health.
- [4] Simon, L. V., & Derebail, V. K. (2021). *Evaluation of the Patient with Lung Disease.* In StatPearls [Internet]. StatPearls Publishing.
- [5] Asif S, Zhao M, Tang F, Zhu Y. A deep learning-based framework for detecting COVID-19 patients using chest X-rays. *Multimed Syst.* 2022;28(4):1495-1513. doi: 10.1007/s00530-022-00917-7. Epub 2022 Mar 22. PMID: 35341212; PMCID: PMC8939400.
- [6] Jain R, Gupta M, Taneja S, Hemanth DJ. Deep learning based detection and analysis of COVID-19 on chest X-ray images. *Appl Intell (Dordr).* 2021;51(3):1690-1700. doi: 10.1007/s10489-020-01902-1. Epub 2020 Oct 9. PMID: 34764553; PMCID: PMC7544769.
- [7] Mahmud T, Rahman M A, Fattah S A. CovXNet: A multi-dilation convolutional neural network for automatic COVID-19 and other pneumonia detection from chest X-ray images with transferable multi-receptive feature optimization[J]. *Computers in biology and medicine*, 2020, 122: 103869.
- [8] Imran, M. A., Posokhova, I., Qureshi, H. N., Masood, U., Riaz, M. S., Ali, K., ... & Hussain, M. (2020). AI4COVID-19: AI enabled preliminary diagnosis for COVID-19 from cough samples via an app. *Informatics in Medicine Unlocked*, 19, 100378.
- [9] K. -C. Chang, J. -W. Huang and Y. -F. Wu, "Design of e-Health System for Heart Rate and Lung Sound Monitoring with AI-based Analysis," 2021 IEEE International Conference on Consumer Electronics-Taiwan (ICCE-TW), Penghu, Taiwan, 2021, pp. 1-2, doi: 10.1109/ICCE-TW52618.2021.9602900.
- [10] Lloyd, Stuart P. "Least squares quantization in PCM." *Information Theory, IEEE*

Transactions on 28.2 (1982): 129-137.

- [11] Radford A, Kim J W, Xu T, et al. Robust speech recognition via large-scale weak supervision[C]//International Conference on Machine Learning. PMLR, 2023: 28492-28518.
- [12] Ke G, Meng Q, Finley T, et al. Lightgbm: A highly efficient gradient boosting decision tree[J]. Advances in neural information processing systems, 2017, 30.
- [13] Rocha B M, Filos D, Mendes L, et al. An open access database for the evaluation of respiratory sound classification algorithms[J]. Physiological measurement, 2019, 40(3): 035001.
- [14] Gulati A, Qin J, Chiu C C, et al. Conformer: Convolution-augmented transformer for speech recognition[J]. arXiv preprint arXiv:2005.08100, 2020.
- [15] LeCun, Y., Bengio, Y. and Hinton, G., 2015. Deep learning. Nature, 521(7553), pp.436-444.
- [16] Vaswani A, Shazeer N, Parmar N, et al. Attention is all you need[J]. Advances in neural information processing systems, 2017, 30.
- [17] Chung J, Gulcehre C, Cho K H, et al. Empirical evaluation of gated recurrent neural networks on sequence modeling[J]. arXiv preprint arXiv:1412.3555, 2014.
- [18] Scikit-learn: Machine Learning in Python, Pedregosa et al., JMLR 12, pp. 2825-2830, 2011.
- [19] Cohen I, Huang Y, Chen J, et al. Pearson correlation coefficient[J]. Noise reduction in speech processing, 2009: 1-4.
- [20] Aranganayagi S, Thangavel K. Clustering categorical data using silhouette coefficient as a relocating measure[C]//International conference on computational intelligence and multimedia applications (ICCIMA 2007). IEEE, 2007, 2: 13-17.
- [21] Chawla N V, Bowyer K W, Hall L O, et al. SMOTE: synthetic minority over-sampling technique[J]. Journal of artificial intelligence research, 2002, 16: 321-357.
- [22] Chen T, Guestrin C. Xgboost: A scalable tree boosting system[C]//Proceedings of the 22nd acm sigkdd international conference on knowledge discovery and data mining. 2016: 785-794.

- [23] Al Daoud E. Comparison between XGBoost, LightGBM and CatBoost using a home credit dataset[J]. *International Journal of Computer and Information Engineering*, 2019, 13(1): 6-10.
- [24] L. Zhang, Y. Zhu, S. Tu and L. Xu, "A Feature Polymerized Based Two-Level Ensemble Model for Respiratory Sound Classification," 2022 IEEE Biomedical Circuits and Systems Conference (BioCAS), Taipei, Taiwan, 2022, pp. 238-242, doi: 10.1109/BioCAS54905.2022.9948561.
- [25] Pham, Lam, et al. "Robust deep learning framework for predicting respiratory anomalies and diseases." 2020 42nd annual international conference of the IEEE engineering in medicine & biology society (EMBC). IEEE, 2020.
- [26] Minami, Koki, et al. "Automatic classification of large-scale respiratory sound dataset based on convolutional neural network." 2019 19th International Conference on Control, Automation and Systems (ICCAS). IEEE, 2019.
- [27] Pham, Lam, et al. "CNN-MoE based framework for classification of respiratory anomalies and lung disease detection." *IEEE journal of biomedical and health informatics* 25.8 (2021): 2938-2947.
- [28] L. Pham, H. Phan, A. Schindler, R. King, A. Mertins and I. McLoughlin, "Inception-Based Network and Multi-Spectrogram Ensemble Applied To Predict Respiratory Anomalies and Lung Diseases," 2021 43rd Annual International Conference of the IEEE Engineering in Medicine & Biology Society (EMBC), Mexico, 2021, pp. 253-256, doi: 10.1109/EMBC46164.2021.9629857.
- [29] Q. Zhang et al., "SPRSound: Open-Source SJTU Paediatric Respiratory Sound Database," in *IEEE Transactions on Biomedical Circuits and Systems*, vol. 16, no. 5, pp. 867-881, Oct. 2022, doi: 10.1109/TBCAS.2022.3204910.
- [30] Pramono, Renard Xaviero Adhi, Stuart Bowyer, and Esther Rodriguez-Villegas. "Automatic adventitious respiratory sound analysis: A systematic review." *PloS one* 12.5 (2017): e0177926.
- [31] Grzywalski, Tomasz, et al. "Practical implementation of artificial intelligence algorithms in pulmonary auscultation examination." *European Journal of Pediatrics* 178 (2019): 883-890.
- [32] Šimundić, Ana-Maria. "Measures of diagnostic accuracy: basic definitions." *ejifcc* 19.4 (2009): 203.
- [33] Zhang Q, Zhang J, Yuan J, et al. Grand challenge on respiratory sound classification for sprsound dataset[C]//2022 IEEE Biomedical Circuits and

- Systems Conference (BioCAS). IEEE, 2022: 213-217.
- [34] Li J, Wang X, Wang X, et al. Improving the resnet-based respiratory sound classification systems with focal loss[C]//2022 IEEE Biomedical Circuits and Systems Conference (BioCAS). IEEE, 2022: 223-227.
- [35] Paszke, Adam, et al. "Pytorch: An imperative style, high-performance deep learning library." *Advances in neural information processing systems* 32 (2019).
- [36] Lin, Tsung-Yi, et al. "Focal loss for dense object detection." *Proceedings of the IEEE international conference on computer vision*. 2017.
- [37] Muda L, Begam M, Elamvazuthi I. Voice recognition algorithms using mel frequency cepstral coefficient (MFCC) and dynamic time warping (DTW) techniques[J]. *arXiv preprint arXiv:1003.4083*, 2010.
- [38] Lewis D D. Naive (Bayes) at forty: The independence assumption in information retrieval[C]//European conference on machine learning. Berlin, Heidelberg: Springer Berlin Heidelberg, 1998: 4-15.
- [39] Cortes C, Vapnik V. Support-vector networks[J]. *Machine learning*, 1995, 20: 273-297.
- [40] Goodfellow, I. et al., 2014. Generative adversarial nets. In *Advances in neural information processing systems*. pp. 2672–2680.
- [41] OpenAI (2023). GPT-4 Technical Report. ArXiv, abs/2303.08774.
- [42] Hendrycks, D. and Gimpel, K. Gaussian error linear units (gelus). *arXiv preprint arXiv:1606.08415*, 2016.
- [43] Child, R., Gray, S., Radford, A., and Sutskever, I. Generating long sequences with sparse transformers. *arXiv preprint arXiv:1904.10509*, 2019.
- [44] Press, O. and Wolf, L. Using the output embedding to improve language models. In *Proceedings of the 15th Conference of the European Chapter of the Association for Computational Linguistics: Volume 2, Short Papers*, pp. 157–163, Valencia, Spain, April 2017. Association for Computational Linguistics. URL <https://aclanthology.org/E17-2025>.
- [45] Sepp Hochreiter and Jürgen Schmidhuber. 1997. Long Short-Term Memory. *Neural Comput.* 9, 8 (November 15, 1997), 1735–1780. <https://doi.org/10.1162/neco.1997.9.8.1735>
- [46] Hsu F S, Huang S R, Huang C W, et al. Benchmarking of eight recurrent neural

network variants for breath phase and adventitious sound detection on a self-developed open-access lung sound database—HF_Lung_V1[J]. PLoS One, 2021, 16(7): e0254134.

[47] Huang S C, Pareek A, Seyyedi S, et al. Fusion of medical imaging and electronic health records using deep learning: a systematic review and implementation guidelines[J]. NPJ digital medicine, 2020, 3(1): 136.

[48] Shwartz-Ziv R, Armon A. Tabular data: Deep learning is not all you need[J]. Information Fusion, 2022, 81: 84-90.

[49] Fraiwan, Mohammad, et al. "A dataset of lung sounds recorded from the chest wall using an electronic stethoscope." Data in Brief 35 (2021): 106913.

ACKNOWLEDGEMENTS

Funding

We express our profound gratitude to the funding organizations that generously supported our research endeavors. Our heartfelt thanks go to the Guangzhou municipal government for bestowing the Basic Science Pilot Award 2023 upon us, significantly facilitating our initial research activities. Additionally, we appreciate the Guangdong Provincial Department of Education for honoring our work with the Education Innovation Project Award 2023. This prestigious accolade not only offered financial support, but also inspired our team to pursue innovative solutions in our field relentlessly. Lastly, we extend our sincere appreciation to the Hong Kong University of Science and Technology (HKUST) Center for Aging Science for their invaluable 2022 Seed Funding (Project number: Z1056). These supports have empowered us to explore novel avenues and broaden our research scope, striving for groundbreaking discoveries in respiratory diseases.

Author contributions

Conceptualization: Pengfei Zhang, Zhihang Zheng, Shaojun Tang. Algorithm development and implementation: Pengfei Zhang. Investigation: Pengfei Zhang, Minghao Yang. Visualization: Pengfei Zhang, Shichen Zhang. Supervision: Shaojun Tang, Pengfei Zhang. Writing—original draft: Pengfei Zhang, Shaojun Tang. Writing—review & editing: Pengfei Zhang, Shaojun Tang, Minghao Yang. All authors approved the final manuscript.

Competing interests

The authors declare no competing interests.

Data and materials availability

The respiratory sound data utilized in this study were sourced from publicly available and well-validated databases, ensuring repeatability and generalization. These databases can be found at the following links:

1. ICBHI Open-Source Respiratory Sound Database: This comprehensive database can be accessed at https://bhichallenge.med.auth.gr/ICBHI_2017_Challenge.

2. Shanghai Jiao Tong University Pediatric Respiratory Sound Database (SPRSound): This open-source pediatric-specific database is available at <https://github.com/SJTU-YONGFU-RESEARCH-GRP/SPRSound>.

3. King Abdullah University Hospital (KAUH) Database: This repository can be found at <https://data.mendeley.com/datasets/jwyy9np4gv/3>.

The codes, pretrained models, and relevant resources for Rene are publicly available with a detailed guide on the GitHub repository: <https://github.com/zpforlove/Rene>. All data needed to evaluate the conclusions in the paper are present in the paper and/or the Supplementary Materials.